Abstracta

Ano XVII - N. 01

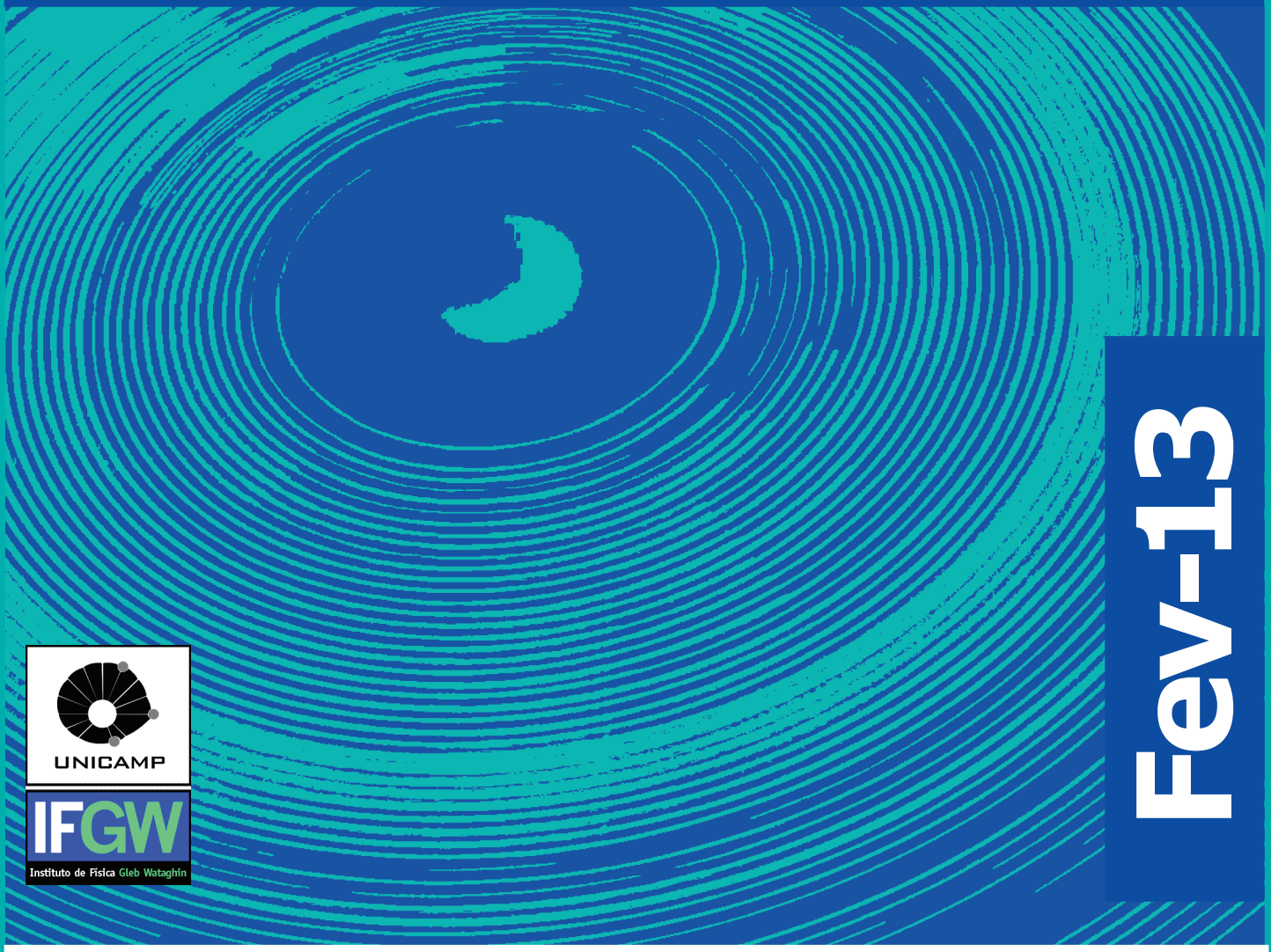

Fev-13

UNICAMP

IFGW
Instituto de Física Gleb Wataghin

Trabalhos Publicados
Novembro 2012 à Fevereiro 2013
P001-13 à P065-13

Proceedings
P066-13

Correções

Defesas de Dissertações do IFGW - D001-13

Defesas de Teses do IFGW - T001-13 à T002-13

Trabalhos Publicados

[P001-2013] "(KsKs0)-K-0 correlations in pp collisions at root s=7 TeV from the LHC ALICE experiment"

Abelev, B.; Adam, J.; Adamova, D.; Adare, A. M.; Aggarwal, M. M.; **Chinellato, D. D.*; Dash, A.*; Takahashi, J.*, et al.**
ALICE Collaboration

Identical neutral kaon pair correlations are measured in root s = 7 TeV pp collisions in the ALICE experiment. One-dimensional (KsKs0)-K-0 correlation functions in terms of the invariant momentum difference of kaon pairs are formed in two multiplicity and two transverse momentum ranges. The femtoscopic parameters for the radius and correlation strength of the kaon source are extracted. The fit includes quantum statistics and final-state interactions of the a(0)/f(0) resonance. (KsKs0)-K-0 correlations show an increase in radius for increasing multiplicity and a slight decrease in radius for increasing transverse mass, mT, as seen in pi pi correlations in pp collisions and in heavy-ion collisions. Transverse mass scaling is observed between the (KsKs0)-K-0 and pi pi radii. Also, the first observation is made of the decay of the f(2)'(1525) meson into the (KsKs0)-K-0 channel in pp collisions.

Physics Review Letters B 717[1-3], 151-161, 2012.

[P002-2013] "A novel method for identifying the local magnetic viscosity process of heterogeneous magnetic nanostructures"

Beron, F.*; de Oliveira, L. A. S.*; Knobel, M.*; Pirota, K. R.*

The relaxation mechanism known as magnetic viscosity has been attracting the attention of the scientific community for more than seven decades. However, a complete model to fully describe the phenomenon is difficult to achieve, owing to its possible different sources and microscopic mechanisms. This work proposes a new experimental approach, based on the combination of static and dynamic first-order reversal curve diagrams. With this technique, one can decouple the responsible mechanism presented by different phases of an inhomogeneous magnetic sample. Moreover, it can also be used to distinguish the microscopic origin of magnetic viscosity (i.e. eddy currents or thermal activation). We successfully applied this novel approach to characterize the local viscosity processes occurring in a nanocrystalline Fe-based soft magnetic ribbon. Owing to the generality of its principles, it can be used to investigate the viscosity of a wide range of systems.

Journal of Physics D-Applied Physics 46[4], 045003, 2013.

[P003-2013] "A Search for Point Sources of EeV Neutrons"

Abreu, P.; Aglietta, M.; Ahlers, M.; Ahn, E. J.; Albuquerque, I. F. M.; Batista, R. Alves; **Chinellato, J. A.*; Daniel, B.*; de Mello Junior, W. J. M.*; Dobrigkeit, C.*; Escobar, C. O.*; Fauth, A. C.*; Kemp, E.*; Muller, M. A.*; Pakk Selmi-Dei, D.*; Silva, M. Z.*; et al.**
Pierre Auger Collaboration

A thorough search of the sky exposed at the Pierre Auger Cosmic Ray Observatory reveals no statistically significant excess of events in any small solid angle that would be indicative of a flux of neutral particles from a discrete source. The search covers from -90 degrees to +15 degrees in declination using four different energy ranges above 1 EeV (10(18) eV). The method used in this search is more sensitive to neutrons than to photons. The upper limit on a neutron flux is derived for a dense grid of directions for each of the four energy ranges. These results constrain scenarios for the production of ultrahigh energy cosmic rays in the Galaxy.

Astrophysical Journal 760[2], 148, 2012.

[P004-2013] "A simple method to obtain Fe-doped CeO2 nanocrystals at room temperature"

Almeida, J. M. A.; Santos, P. E. C.; Cardoso, L. P.; **Meneses, C. T.***

Ce1-xFexO2 nanocrystals (0 < x < 0.05) have been synthesized at room temperature using the coprecipitation method. The samples were characterized by X-ray powder diffraction (XRD), transmission electron microscopy (TEM) and magnetization measurements as a function of field. The XRD results and Rietveld refinement analysis show that all particles have a crystalline structure isomorphous to the host structure (CeO2), with average size of 9 nm. This information was also confirmed by TEM images in which it is shown that the particles present spherical-like shape. The magnetic measurements indicated that the Fe-doped samples exhibit a weak ferromagnetism at room temperature, which increases with the increasing of the Fe content.

Journal of Magnetism and Magnetic Materials 327[185-188], 2013.

[P005-2013] "Ampegravere's motor: Its history and the controversies surrounding its working mechanism"

Assis, A. K. T.*; Chaib, J. P. M. C.

In 1822 Ampere created a new kind of motor when he succeeded in spinning a cylindrical magnet around its axis by connecting it to a battery generating a steady current. Nowadays, it is easy to present such a motor in the classroom utilizing a neodymium magnet, a D battery, a steel nail, and a short piece of copper wire. Although it is very simple to observe the rotation, the explanation of this effect is still under dispute. This work presents the history of this motor including the controversy between Ampere and Faraday, as well as the modern explanation based on the field concept. We emphasize the positive outcomes to be gained in the classroom by presenting this device to students.

American Journal of Physics 80[11], 990-995, 2012.

[P006-2013] "Anomalous centrality evolution of two-particle angular correlations from Au-Au collisions at root s(NN)=62 and 200 GeV"

Agakishiev, G.; Aggarwal M. M.; Ahammed, Z.; Alakhverdyants, A. V.; Alekseev I.; **Derradi de Souza, R.*; Takahashi, J.*; Vasconcelos, G. M. S.*; et al.**
STAR Collaboration

We present two-dimensional (2D) two-particle angular correlations measured with the STAR detector on relative pseudorapidity eta and azimuth phi for charged particles from Au-Au collisions at root s(NN) = 62 and 200 GeV with transverse momentum p(t) >= 0.15 GeV/c, vertical bar eta vertical bar <= 1, and 2 pi in azimuth. Observed correlations include a same-side (relative azimuth <pi/2) 2D peak, a closely related away-side azimuth dipole, and an azimuth quadrupole conventionally associated with elliptic flow. The same-side 2D peak and away-side dipole are explained by semihard parton scattering and fragmentation (minijets) in proton-proton and peripheral nucleus-nucleus collisions. Those structures follow N-N binary-collision scaling in Au-Au collisions until midcentrality, where a transition to a qualitatively different centrality trend occurs within one 10% centrality bin. Above the transition point the number of same-side and away-side correlated pairs increases rapidly relative to binary-collision scaling, the eta width of the same-side 2D peak also increases rapidly (eta elongation), and the phi width actually decreases significantly. Those centrality trends are in marked contrast with conventional expectations for jet quenching in a dense medium. The observed centrality trends are compared to perturbative QCD predictions computed in HIJING, which serve as a theoretical baseline, and to the expected trends for semihard parton scattering and fragmentation in a thermalized opaque medium predicted by theoretical calculations and phenomenological models.

We are unable to reconcile a semihard parton scattering and fragmentation origin for the observed correlation structure and centrality trends with heavy-ion collision scenarios that invoke rapid parton thermalization. If the collision system turns out to be effectively opaque to few-GeV partons the present observations would be inconsistent with the minijet picture discussed here.

Physical Review C 86[6], 064902, 2012.

[P007-2013] "Antennas for the detection of radio emission pulses from cosmic-ray induced air showers at the Pierre Auger Observatory"

Abreu, P.; Aglietta, M.; Ahlers, M.; Ahn, E. J.; Albuquerque, I. F. M.; **Alves Batista, R.*; Chinellato, J. A.*; de Mello Junior, W. J. M.*; Dobrigkeit, C.*; Escobar, C. O.*; Fauth, A. C.*; Kemp, E.*; Muller, M. A.*; Pakk Selmi-Dei, D.*; Zimbres, S. M.*; et al.** Pierre Auger Collaboration

The Pierre Auger Observatory is exploring the potential of the radio detection technique to study extensive air showers induced by ultra-high energy cosmic rays. The Auger Engineering Radio Array (AERA) addresses both technological and scientific aspects of the radio technique. A first phase of AERA has been operating since September 2010 with detector stations observing radio signals at frequencies between 30 and 80 MHz. In this paper we present comparative studies to identify and optimize the antenna design for the final configuration of AERA consisting of 160 individual radio detector stations. The transient nature of the air shower signal requires a detailed description of the antenna sensor. As the ultra-wideband reception of pulses is not widely discussed in antenna literature, we review the relevant antenna characteristics and enhance theoretical considerations towards the impulse response of antennas including polarization effects and multiple signal reflections. On the basis of the vector effective length we study the transient response characteristics of three candidate antennas in the time domain. Observing the variation of the continuous galactic background intensity we rank the antennas with respect to the noise level added to the galactic signal.

Journal of Instrumentation 7, P10011, 2012.

[P008-2013] "Are HFC buses a feasible alternative for urban transportation in Paraguay?"

Espinola, M. O. G.; **da Silva, E. P.***; Camargo, J. C.

Paraguay is very rich in hydropower and a net importer of fossil fuels. Besides, in Paraguay, the transportation sector counts for a big share of the total energy demand. So if this sector would be changed to clean fuel, imported oil dependence and air pollution will be reduced dramatically. This paper assesses the feasibility of HFC urban buses implementation in the transportation sector in Paraguay. In general, annual transportation cost for a fleet of 55 HFC urban buses is estimated in US$ 33,682,581 compared with US$ 40,612,741.84 for diesel urban buses, which indicates that this technology could be an economical and environmentally clean alternative to substitute diesel urban buses in the Paraguayan transportation sector. These results are strongly linked to the chosen boundary conditions, such as electricity price and availability, the electrolytic hydrogen demand and the basic electrolyser's management.

International Journal of Hydrogen Energy 37[21], 16177-16185, 2012.

[P009-2013] "Biofuel production from water hyacinth in the Pantanal wetland"

Bergier, I.; Salis, S. M.; Miranda, C. H. B.; Ortega, E.; **Luengo, C. A.***

The Pantanal is a major wetland in the inner South America, with the potential for production of large quantities of biomass of aquatic floating species, especially water hyacinth (Eicchornia crassipes and E. azurea), during the aquatic phase of the floodpulse characteristic for this ecosystem. Such biomass could be wisely managed for the production of biofuels. This should be based on the concepts of renewability and ecosystem surplus, and could help in neutralizing of regional and global industrial carbon impacts and to induce socioeconomic development. The aquatic biomass exploitation would require low fossil energy and materials inputs, leaving a positive energy balance, with minimal interference in the environment. This emerging biofuel-based economy in the Pantanal can be a good example of human adaptation to climatic changes by managing carbon export of natural wetlands. The concepts described herein could be used in other natural, restored or artificially constructed wetlands.

Ecohydrology and Hydrobiology 12[1], 77-84, 2012.

[P010-2013] "Brain plasticity for verbal and visual memories in patients with mesial temporal lobe epilepsy and hippocampal sclerosis: An fMRI study"

Alessio, A.*; Pereira, F. R. S.; **Sercheli, M. S.*; Rondina, J. M.*; Ozelo, H. B.*;** Bilevicius, E.; Pedro, T.; **Covolan, R. J. M.*;** Damasceno, B. P.; Cendes, F.

We aimed to identify the brain areas involved in verbal and visual memory processing in normal controls and patients with unilateral mesial temporal lobe epilepsy (MTLE) associated with unilateral hippocampal sclerosis (HS) by means of functional magnetic resonance imaging (fMRI). The sample comprised nine normal controls, eight patients with right MTLE, and nine patients with left MTLE. All subjects underwent fMRI with verbal and visual memory paradigms, consisting of encoding and immediate recall of 17 abstract words and 17 abstract drawings. A complex network including parietal, temporal, and frontal cortices seems to be involved in verbal memory encoding and retrieval in normal controls. Although similar areas of activation were identified in both patient groups, the extension of such activations was larger in the left-HS group. Patients with left HS also tended to exhibit more bilateral or right lateralized encoding related activations. This finding suggests a functional reorganization of verbal memory processing areas in these patients due to the failure of left MTL system. As regards visual memory encoding and retrieval, our findings support the hypothesis of a more diffuse and bilateral representation of this cognitive function in the brain. Compared to normal controls, encoding in the left-HS group recruited more widespread cortical areas, which were even more widespread in the right-HS group probably to compensate for their right mesial temporal dysfunction. In contrast, the right-HS group exhibited fewer activated areas during immediate recall than the other two groups, probably related to their greater difficulty in dealing with visual memory content.

Human Brain Mapping 34[1], 186-199, 2013.

[P011-2013] "Charge separation relative to the reaction plane in Pb-Pb collisions at root s(NN)=2.76 TeV"

Abelev, B.; Adam, J.; Adamova, D.; Adare, A. M.; Aggarwal, M. M.; **Chinellato, D. D.*; Dash, A.*; Takahashi, J.*; et al.** ALICE Collaboration

Measurements of charge-dependent azimuthal correlations with the ALICE detector at the LHC are reported for Pb-Pb collisions at root s(NN) = 2.76 TeV. Two- and three-particle charge-dependent azimuthal correlations in the pseudorapidity range vertical bar eta vertical bar < 0.8 are presented as a function of the collision centrality, particle separation in pseudorapidity, and transverse momentum. A clear signal compatible with a charge-dependent separation relative to the reaction plane is observed, which shows little or no collision energy dependence when compared to measurements at RHIC energies.

This provides a new insight for understanding the nature of the charge-dependent azimuthal correlations observed at RHIC and LHC energies.

Physical Review Letters 110[1], 012301, 2013.

[P012-2013] "Coarse-graining scale and effectiveness of hydrodynamic modeling"

Mota, Ph.; Kodama, T.; **de Souza, R. D.*; Takahashi, J.***

Some basic questions about the hydrodynamical approach to relativistic heavy-ion collisions are discussed aiming to clarify how far we can go with such an approach to extract useful information on the properties and dynamics of the QCD matter created. We emphasize the importance of the coarse-graining scale required for the hydrodynamic modeling which determines the space-time resolution and the associated limitations of collective flow observables. We show that certain kinds of observables can indicate the degree of inhomogeneity of the initial condition under less stringent condition than the local thermal equilibrium subjected to the coarse-graining scale compatible to the scenario.

European Physical Journal A 48[11], 165, 2012.

[P013-2013] "Constraining sterile neutrinos with AMANDA and IceCube atmospheric neutrino data"

Esmaili, A.*; Halzen, F.; **Peres, O. L. G.***

We demonstrate that atmospheric neutrino data accumulated with the AMANDA and the partially deployed IceCube experiments constrain the allowed parameter space for a hypothesized fourth sterile neutrino beyond the reach of a combined analysis of all other experiments, for Delta m(41) (2) less than or similar to 1 eV(2). Although the IceCube data wins the statistics in the analysis, the advantage of a combined analysis of AMANDA and IceCube data is the partial remedy of yet unknown instrumental systematic uncertainties. We also illustrate the sensitivity of the completed IceCube detector, that is now taking data, to the parameter space of 3+1 model.

Journal of Cosmology and Astroparticle Physics [11], 041, 2012.

[P014-2013] "Constraints on the Origin of Cosmic Rays Above 10(18) eV from Large-scale Anisotropy Searches in data of the Pierre Auger Observatory"

Abreu, P.; Aglietta, M.; Ahlers, M.; Ahn, E. J.; Albuquerque, I. F. M.; Allard, D.; **Alves Batista, R.*; Chinellato, J. A.*; Daniel, B.*; de Mello, W. J. M., Jr.*; Dobrigkeit, C.*; Escobar, C. O.*; Fauth, A. C.*; Kemp, E.*; Muller, M. A.*; Selmi-Dei, D. Pakk*; Zimbres Silva, M.*; et al.**
Pierre Auger Collaboration

A thorough search for large-scale anisotropies in the distribution of arrival directions of cosmic rays detected above 10(18) eV at the Pierre Auger Observatory is reported. For the first time, these large-scale anisotropy searches are performed as a function of both the right ascension and the declination and expressed in terms of dipole and quadrupole moments. Within the systematic uncertainties, no significant deviation from isotropy is revealed. Upper limits on dipole and quadrupole amplitudes are derived under the hypothesis that any cosmic ray anisotropy is dominated by such moments in this energy range. These upper limits provide constraints on the production of cosmic rays above 10(18) eV, since they allow us to challenge an origin from stationary galactic sources densely distributed in the galactic disk and emitting predominantly light particles in all directions.

Astrophysical Journal Letters 762[1], L13, 2013.

[P015-2013] "Curvature and Temperature Discrimination Using Multimode Interference Fiber Optic Structures-A Proof of Concept"

Silva, S.; **Pachon, E. G. P.***; Franco, M. A. R.; Jorge, P.; Santos, J. L.; Malcata, F. X.; **Cordeiro, C. M. B.***; Frazao, O.

Singlemode-multimode-singlemode fiber structures (SMS) based on distinct sections of a pure silica multimode fiber (coreless-MMF) with diameters of 125 and 55 mu m, were reported for the measurement of curvature and temperature. The sensing concept relies on the multimode interference that occurs in the coreless-MMF section and, in accordance with the length of the MMF section used, two fiber devices were developed: one based on a bandpass filter (self-image effect) and the other on a band-rejection filter. Maximum sensitivities of 64.7 nm.m and 13.08 pm/degrees C could be attained, for curvature and temperature, respectively, using the band-rejection filter with 55 mu m-MMF diameter. A proof of concept was also explored for the simultaneous measurement of curvature and temperature by means of the matrix method.

Journal of Lightwave Technology 30[23], 3569-3575, 2012.

[P016-2013] "D-S(+) meson production at central rapidity in proton-proton collisions at root s=7 TeV"

Abelev, B.; Adam, J.; Adamova, D.; Adare, A. M.; Aggarwal, M. M.; **Chinellato, D. D.*; Dash, A.*; Takahashi, J.*; et al.**
ALICE Collaboration

The P-T-differential inclusive production cross section of the prompt charm-strange meson D-s(+) in the rapidity range vertical bar y vertical bar < 0.5 was measured in proton-proton collisions at root s = 7 TeV at the LHC using the ALICE detector. The analysis was performed on a data sample of 2.98 x 10(8) events collected with a minimum-bias trigger. The corresponding integrated luminosity is L-int = 4.8 nb(-1). Reconstructing the decay D-s(+) -> phi pi(+) with phi -> K-K+, and its charge conjugate, about 480 D-s(+/-) mesons were counted, after selection cuts, in the transverse momentum range 2 < P-T < 12 GeV/c. The results are compared with predictions from models based on perturbative QCD. The ratios of the cross sections of four D meson species (namely D-0, D+, D*+ and D-s(+)) were determined both as a function of p(T) and integrated over p(T)after extrapolating to full p(T) range, together with the strangeness suppression factor in charm fragmentation. The obtained values are found to be compatible within uncertainties with those measured by other experiments in e(+) e(-), ep and pp interactions at various centre-of-mass energies.

Physics Letters B 718[2], 279-294, 2012.

[P017-2013] "Direct measurement of backgrounds using reactor-off data in Double Chooz"

Abe, Y.; Aberle, C.; dos Anjos, J. C.; Barriere, J. C.; Bergevin, M.; **Gonzalez, L. F. G.*; Kemp, E.***; et al.
Double Chooz Collaboration

Double Chooz is unique among modern reactor-based neutrino experiments studying (nu) over bar (e) disappearance in that data can be collected with all reactors off. In this paper, we present data from 7.53 days of reactor-off running. Applying the same selection criteria as used in the Double Chooz reactor-on oscillation analysis, a measured background rate of 1.0 +/- 0.4 events/day is obtained. The background model for accidentals, cosmogenic beta-n-emitting isotopes, fast neutrons from cosmic muons, and stopped-mu decays used in the oscillation analysis is demonstrated to be correct within the uncertainties. Kinematic distributions of the events, which are dominantly cosmic-ray-produced correlated-background events, are provided. The background rates are scaled to the shielding depths of two other reactor-based oscillation experiments, Daya Bay and RENO.

Physical Review D 87[1], 011102, 2013.

[P018-2013] "Effects of Cr3+ concentration on the optical properties of Cs2NaAlF6 single crystals"

Pedro, S. S.; Sosman, L. P.; Barthem, R. B.; **Tedesco, J. C. G.*;** Bordallo, H. N.

This work is devoted to the study of optical properties of the elpasolite Cs2NaAlF6 with 0.1, 1.0, 3.0, 10.0, 30.0 and 50.0% of Cr3+ ions. The interest in this system lies on the fact that it presents a high quantum yield in the visible and infrared regions and therefore can be considered for laser applications. The photoluminescence and excitation spectra were obtained at 5 and 300 K, while the absorption spectra were measured at 300 K. The spectra at 300 K show broad bands attributed to the Cr3+ ions in two non-equivalent sites, both of them with octahedral coordination, while at 5 K we can observe the vibrational modes of the [CrF6] (3-) complex. The ensemble of our results lead us to conclude that the material has potential applications as a lasing system.

Journal of Luminescence 134, 100-106, 2013.

[P019-2013] "Electrically, Chemically, and Photonically Powered Torsional and Tensile Actuation of Hybrid Carbon Nanotube Yarn Muscles"

Lima, M. D.; Li, N.; de Andrade, M. J.; Fang, S. L.; Oh, J.; Spinks, G. M.; Kozlov, M. E.; Haines, C. S.; Suh, D.; Foroughi, J.; Kim, S. J.; Chen, Y. S.; Ware, T.; Shin, M. K.; **Machado, L. D.***; Fonseca, A. F.; Madden, J. D. W.; Voit, W. E.; **Galvao, D. S.***; Baughman, R. H.

Artificial muscles are of practical interest, but few types have been commercially exploited. Typical problems include slow response, low strain and force generation, short cycle life, use of electrolytes, and low energy efficiency. We have designed guest-filled, twist-spun carbon nanotube yarns as electrolyte-free muscles that provide fast, high-force, large-stroke torsional and tensile actuation. More than a million torsional and tensile actuation cycles are demonstrated, wherein a muscle spins a rotor at an average 11,500 revolutions/minute or delivers 3% tensile contraction at 1200 cycles/minute. Electrical, chemical, or photonic excitation of hybrid yarns changes guest dimensions and generates torsional rotation and contraction of the yarn host. Demonstrations include torsional motors, contractile muscles, and sensors that capture the energy of the sensing process to mechanically actuate.

Science 338[6109], 928-932, 2012.

[P020-2013] "Emergence of the Pointer Basis through the Dynamics of Correlations"

Cornelio, M. F.N*; Farias O. J.; Fanchini F. F.; Frerot, I.; Aguilar, G. H.; Hor-Meyll, M. O.; **de Oliveira, M. C.***; Walborn, S. P.; **Caldeira, A. O.***; Ribeiro P. H. S.

We use the classical correlation between a quantum system being measured and its measurement apparatus to analyze the amount of information being retrieved in a quantum measurement process. Accounting for decoherence of the apparatus, we show that these correlations may have a sudden transition from a decay regime to a constant level. This transition characterizes a nonasymptotic emergence of the pointer basis, while the system apparatus can still be quantum correlated. We provide a formalization of the concept of emergence of a pointer basis in an apparatus subject to decoherence. This contrast of the pointer basis emergence to the quantum to classical transition is demonstrated in an experiment with polarization entangled photon pairs.

Physical Review Letters 109[19], 190402, 2012.

[P021-2013] "Fabrication and upconversion luminescence of Er3+/Yb3+ codoped TeO2-WO3-Na2O-Nb2O5-Al2O3 glass fibers"

Narro-Garcia, R.*; Chillcce, E. F.*; Barbosa, L. C.*; de Posada, E.; Arronte, M.; Rodriguez, E.

The tellurite fibers based on glasses with the composition TeO2-WO3-Nb2O5-Na2O-Al2O3-Er2O3-Yb2O3 were fabricated by the rod-in-tube technique using a Heathway drawing tower. The upconversion luminescence of Er3+/Yb3+ codoped tellurite glass fibers under 980 nm excitation were investigated. The Er3+/Yb(3+)co-doped tellurite fibers show an efficient up-conversion process in comparison with the Er3+-doped tellurite fibers. The pump power dependent intensities were discussed, which showed that two photons are involved in the upconversion process.

Journal of Luminescence 134, 528-532, 2013.

[P022-2013] "Ferroic states and phase coexistence in BiFeO3-BaTiO3 solid solutions"

Gotardo, R. A. M.; Viana, D. S. F.; Olzon-Dionysio, M.; Souza, S. D.; Garcia, D.; Eiras, J. A.; Alves, M. F. S.; Cotica, L. F.; Santos, I. A.; **Coelho, A. A.***

In this paper structural, electric, magnetic, and Mossbauer spectroscopy studies were conducted in (x) BiFeO3-(1-x) BaTiO3, 0.9 >= x >= 0.3, solid solutions. X-ray diffraction and Rietveld refinement studies indicated the formation of single-phased materials crystallized in a distorted perovskite structure with the coexistence of rhombohedral and monoclinic symmetries. Room temperature ferroelectric hysteresis loops showed that the electric polarization increases with the increase of the BaTiO3 content due to the singular structural evolution of the studied solid solutions. All samples presented weak ferromagnetic ordering, which indicates that the BaTiO3 substitution in the BiFeO3 matrix released the latent magnetization. Mossbauer studies revealed a magnetic spectral signature corresponding to ordered Fe3+ ions, and a decrease of the magnetic hyperfine magnetic fields with the increase of the BaTiO3 content. The composition 0.3BiFeO(3)-0.7BaTiO(3) presented a spectral signature corresponding to a paramagnetic behavior, which strongly suggests that the observed magnetization in this sample is due to the Ti3+ ions.

Journal of Applied Physics 112[10], 104112, 2012.

[P023-2013] "First order reversal curve analysis on NdFeB nanocomposite ribbons subjected to Joule heating treatments"

Pampillo, L. G.; Saccone, F. D.; **Knobel, M.*;** Sirkin, H. R. M.

Amorphous precursors with composition Nd4.5Fe72-xCo3+xCr2Al1B17.5 (x = 0, 2, 7, 12) were thermally treated by the Joule heating technique with a linearly varying electrical current. The crystallization kinetics was followed by monitoring the resistance of the ribbons during the heating up to the final applied current. Crystallized nanostructured phases coexist with an amorphous matrix, as it was observed by means of Mossbauer Spectroscopy and X-ray diffraction. The irreversible magnetic response of the Joule heated ribbons was analyzed by the First Order Reversal Curves (FORC) diagram technique. For the optimal treatments, associated with the higher maximum energy products for each sample composition, it was found that the main interaction is of a strongly dipolar characteristic. Over annealed samples show a FORC diagram that gives into account of softening, due to grain growth, for those phases precipitated at the first crystallization stage. When it is measured at 20 K, the hardest magnetic sample (Fe = 72 at.%, Co = 3 at.%, I-final = 0.5 A), exhibits a diagram with characteristics corresponding to dipolar interactions of soft phases. This fact is consistent with an enhancement of the exchange length due to the increase in the soft phase stiffness as it is expected at low temperatures.

Journal of Alloys and Compounds 536, S389-S393, Suplemento 1, 2012.

[P024-2013] "First test of Lorentz violation with a reactor-based antineutrino experiment"

Abe, Y.; Aberle, C.; dos Anjos, J. C.; Bergevin, M.; Bernstein , A.; **Gonzalez, L. F. G.*; Kemp, E.*; Valdiviesso, G.*; et al.**
Double Chooz Collaboration

We present a search for Lorentz violation with 8249 candidate electron antineutrino events taken by the Double Chooz experiment in 227.9 live days of running. This analysis, featuring a search for a sidereal time dependence of the events, is the first test of Lorentz invariance using a reactor-based antineutrino source. No sidereal variation is present in the data and the disappearance results are consistent with sidereal time independent oscillations. Under the Standard-Model Extension, we set the first limits on 14 Lorentz violating coefficients associated with transitions between electron and tau flavor, and set two competitive limits associated with transitions between electron and muon flavor.

Physical Review D 86[11], 112009, 2012.

[P025-2013] "Graphene to fluorographene and fluorographane: a theoretical study"

Paupitz, R.; **Autreto, P. A. S.***; Legoas, S. B.; Srinivasan, S. G.; van Duin, T.; **Galvao, D. S.***

We report here a fully reactive molecular dynamics study on the structural and dynamical aspects of the fluorination of graphene membranes (fluorographene). Our results show that fluorination tends to produce defective areas on the graphene membranes with significant distortions of carbon-carbon bonds. Depending on the amount of incorporated fluorine atoms, large membrane holes were observed due to carbon atom losses. These results may explain the broad distribution of the structural lattice parameter values experimentally observed. We have also investigated the effects of mixing hydrogen and fluorine atoms on the graphene functionalization. Our results show that, when in small amounts, the presence of hydrogen atoms produces a significant decrease in the rate of fluorine incorporation onto the membrane. On the other hand, when fluorine is the minority element, it produces a significant catalytic effect on the rate of hydrogen incorporation. We have also observed the spontaneous formation of new hybrid structures with different stable configurations (chair-like, zigzag-like and boat-like) which we named fluorographane. S Online supplementary data available from stacks.iop.org/Nano/24/035706/mmedia.

Nanotechnology 24[3], 035706, 2013.

[P026-2013] "High fidelity and flexible quantum state transfer in the atom-coupled cavity hybrid system"

Yabu-uti, B. F. C.*; Roversi, J. A.*

We investigate a system composed of N coupled cavities (linear array) and two-level atoms interacting one at a time. Adjusting appropriately the atom-field detuning, and making the hopping rate of photons between neighboring cavities, A, greater than the atom-field coupling g (i.e. A >> N (3/2) g), we can eliminate the interaction of the atom with the non-resonant normal modes reducing the dynamics to the interaction of the atom with only a single-mode. As an application of this interaction, we propose a two-step protocol for quantum communication of an arbitrary atomic quantum state between distant coupled cavities. In the ideal case, the coupled cavities system acts as a perfect quantum bus and we obtain a flexible and perfect quantum communication for any N. Considering the influence of dissipation, an interesting parity effect emerges and we still obtain a high fidelity quantum state transfer for an appreciable number of cavities with current experimental parameters. We also studied important sources of imperfections during the procedure.

Quantum Information Processing 12[1], 189-204, 2013.

[P27-2013] "High sensitivity LPG Mach-Zehnder sensor for real-time fuel conformity analysis"

Osorio, J. H.*; Mosquera, L.*; Gouveia, C. J.; **Biazoli, C. R.*; Claudecir, R.*; Hayashi, J. G.*;** Jorge, P. A. S.; **Juliano, G.*; Cordeiro, C. M. B.***

A high sensitivity refractive index sensor based on the combination of mechanically induced long period gratings (LPG) and fiber tapers was developed for real-time fuel quality analysis. The sensor was built in a Mach-Zehnder configuration by employing a pair of in-series gratings. In order to enhance sensor sensitivity, the region between both LPGs was tapered down from 125 to 10 mu m. The system was tested by measuring water concentration in ethanol and ethanol concentration in commercial gasoline. The tapered sensor has shown an average sensitivity of 930 nm/RIU, 18 times higher than the non-tapered version. The resolution limit of the system using spectral interrogation was estimated to be 0.06% of ethanol dissolved in gasoline. For the purpose of real-time monitoring, an interrogation system based on white light interferometry (WLI) and virtual instrumentation was employed to evaluate ethanol evaporation in water, avoiding the use of spectral analysis. The WLI system, using phase tracking techniques, enabled us to record the evolution of the ethanol concentration in water with a resolution of 0.005% (v/v).

Measurement Science & Technology 24[1], 015102, 2013.

[P028-2013] "Impacts of enemy-mediated effects and the additivity of interactions in an insect trophic system"

Reigada, C.*; Araujo, S. B. L.; **de Aguiar, M.*; Aloizio, M.*;** Giao, J. Z.; Guimaraes, P. R.; Trinca, L. A.; Godoy, W. A. C.

In this study, we used data from both experiments and mathematical simulations to analyze the consequences of the interacting effects of intraguild predation (IGP), cannibalism and parasitism occurring in isolation and simultaneously in trophic interactions involving two blowfly species under shared parasitism. We conducted experiments to determine the short-term response of two blowfly species to these interactions with respect to their persistence. A mathematical model was employed to extend the results obtained from these experiments to the long-term consequences of these interactions for the persistence of the blowfly species. Our experimental results revealed that IGP attenuated the strength of the effects of cannibalism and parasitism between blowfly host species, increasing the probability of persistence of both populations. The simulations obtained from the mathematical model indicated that IGP is a key interaction for the long-term dynamics of this system. The presence of different species interacting in a tri-trophic system relaxed the severity of the effects of a particular interaction between two species, changing species abundances and promoting persistence through time. This pattern was related to indirect interactions with a third species, the parasitoid species included in this study.

Population Ecology 55[1], 11-26, 2013.

[P029-2013] "Implications of the pseudo-Dirac scenario for ultra high energy neutrinos from GRBs"

Esmaili, A.*; Farzan, Y.

The source of Ultra High Energy COSillic Rays (ULIECR) is still en unresolved mystery. Up until recently, sources of Gamma Ray Bursts (GRBs) had been considered as a suitable source for UHECR.

Within the fireball model, the UHECR produced at GRBs should be accompanied with a neutrino flux detectable at the neutrino telescope such as IceCube. Recently, IceCube has set an upper bound on the neutrino flux accompanied by GRBs about 3.7 times below the prediction. We investigate whether this deficit can be explained by the oscillation of the active neutrinos to sterile neutrinos en route from the source to the detectors within the pseudo-Dirac scenario. We then discuss the implication of this scenario for diffuse supernova relic neutrinos.

Journal of Cosmology and Astroparticle Physics [12], 014, 2012.

[P030-2013] "Inclusive charged hadron elliptic flow in Au+Au collisions at root s(NN)=7.7-39 GeV"

Adamczyk, L.; Agakishiev, G.; Aggarwal, M. M.; Ahammed, Z.; Alakhverdyants, A. V.; **Derradi de Souza, R.*; Takahashi, J.*; Vasconcelos, G. M. S.*; et al.**
STAR Collaboration

A systematic study is presented for centrality, transverse momentum (p(T)), and pseudorapidity (eta) dependence of the inclusive charged hadron elliptic flow (v(2)) at midrapidity (vertical bar eta vertical bar < 1.0) in Au + Au collisions at root s(NN) = 7.7, 11.5, 19.6, 27, and 39 GeV. The results obtained with different methods, including correlations with the event plane reconstructed in a region separated by a large pseudorapidity gap and four-particle cumulants (v(2){4}), are presented to investigate nonflow correlations and v(2) fluctuations. We observe that the difference between v(2){2} and v(2){4} is smaller at the lower collision energies. Values of v(2), scaled by the initial coordinate space eccentricity, v(2)/epsilon, as a function of p(T) are larger in more central collisions, suggesting stronger collective flow develops in more central collisions, similar to the results at higher collision energies. These results are compared to measurements at higher energies at the Relativistic Heavy Ion Collider (root s(NN) = 62.4 and 200 GeV) and at the Large Hadron Collider (Pb + Pb collisions at root s(NN) = 2.76 TeV). The v(2)(pT) values for fixed pT rise with increasing collision energy within the pT range studied (<2 GeV/c). A comparison to viscous hydrodynamic simulations is made to potentially help understand the energy dependence of v(2)(pT). We also compare the v(2) results to UrQMD and AMPT transport model calculations, and physics implications on the dominance of partonic versus hadronic phases in the system created at beam energy scan energies are discussed.

Physical Review C 86[5], 054908, 2012.

[P031-2013] "Inclusive J/psi production in pp collisions at root s=2.76 TeV"

Abelev, B.; Adam, J.; Adamova, D.; Adare, A. M.; Aggarwal M. M.; **Chinellato, D. D.*; Cosentino, M. R.*; Dash, A.*; Takahashi, J.*, et al.**
ALICE Collaboration

The ALICE Collaboration has measured inclusive J/psi production in pp collisions at a center-of-mass energy root s = 2.76 TeV at the LHC. The results presented in this Letter refer to the rapidity ranges vertical bar y vertical bar < 0.9 and 2.5 < y <4 and have been obtained by measuring the electron and muon pair decay channels, respectively. The integrated luminosities for the two channels are L-int(e) = 1.1 nb(-1) and L-int(mu) = 19.9 nb(-1), and the corresponding signal statistics are N-J/psi(e+e-) = 59 +/- 14 and N-J/psi(mu+mu-) = 1364 +/- 53. We present d sigma(J/psi)/dy for the two rapidity regions under study and, for the forward-y range, d(2)sigma(J/psi)/dydp(t) in the transverse momentum domain 0 < p(t) < 8 GeV/c. The results are compared with previously published results at root s = 7 TeV and with theoretical calculations.

Physics Letters B 718[2], 295-306, 2012.

[P032-2013] "Intensity curvature sensor based on photonic crystal fiber with three coupled cores"

Martins, H.; Marques, M. B.; Jorge, P.; **Cordeiro, C. M. B.***; Frazao, O.

An intensity curvature sensor using a Photonic Crystal Fiber (PCF) with three coupled cores is proposed. The three cores were aligned and there was an air hole between each two consecutive cores. The fiber had a low air filling fraction, which means that the cores remain coupled in the wavelength region studied. Due to this coupling, interference is obtained in the fiber output even if just a single core is illuminated. A configuration using reflection interrogation, which used a section fiber with 0.13 m as the sensing head, was characterized for curvature sensing. When the fiber is bended along the plane of the cores, one of the lateral cores will be stretched and the other compressed. This changes the coupling coefficient between the three cores, changing the output optical power intensity. The sensitivity of the sensing head was strongly dependent on the direction of bending, having its maximum when the bending direction was along the plane of the cores. A maximum curvature sensitivity of 2.0 dB/m(-1) was demonstrated between 0 m and 2.8 m.

Optics Communications 285[24], 5128-5131, 2012.

[P033-2013] "Large-scale Distributionj of Arrival Directions of Cosmic Rays Detected Above 10(18) eV at the Pierre Auger Observatory"

Abreu, P.; Aglietta, M.; Ahlers, M.; Ahn, E. J.; Albuquerque, I. F. M.; **Batista, R. A.*; Chinellato, J. A.*; Daniel, B.*; de Mello Junior, W. J. M.*; Dobrigkeit, C.*; Escobar, C. O.*; Fauth, A. C.*; Kemp, E.*; Muller, M. A.*; Selmi-Dei, D. Pakk*; Silva, M. Z.*; et al.**
Pierre Auger Collaboration

A thorough search for large-scale anisotropies in the distribution of arrival directions of cosmic rays detected above 10(18) eV at the Pierre Auger Observatory is presented. This search is performed as a function of both declination and right ascension in several energy ranges above 10(18) eV, and reported in terms of dipolar and quadrupolar coefficients. Within the systematic uncertainties, no significant deviation from isotropy is revealed. Assuming that any cosmic-ray anisotropy is dominated by dipole and quadrupole moments in this energy range, upper limits on their amplitudes are derived. These upper limits allow us to test the origin of cosmic rays above 10(18) eV from stationary Galactic sources densely distributed in the Galactic disk and predominantly emitting light particles in all directions.

Astrophysical Journal Supplement Series 203[2], 34, 2012.

[P034-2013] "Light intensity dependent Debye screening length in undoped photorefractive titanosillenite crystals"

de Oliveira I.; **Frejlich J.***

We report on the experimental evidence of the light intensity dependence of the Debye screening length l(s) in undoped photorefractive titanosillenite crystals (Bi12TiO20) by measuring the holographic gain and diffraction efficiency in a two-wave mixing experiment under 532 nm wavelength laser light. Debye length shows saturation at high values of the light intensity. Results are in agreement with the theoretical development.

Journal of Applied Physics 112[11], 113523, 2012.

[P035-2013] "Low-energy electron scattering by cellulose and hemicellulose components"

de Oliveira E. M.; da Costa R. F.; Sanchez S. D.; Natalense A. P. P.; Bettega M. H. F.; **Lima M. A. P.***; Varella M. T. D.

We report elastic integral, differential and momentum transfer cross sections for low-energy electron scattering by the cellulose components beta-D-glucose and cellobiose (beta(1 -> 4) linked glucose dimer), and the hemicellulose component beta-D-xylose. For comparison with the b forms, we also obtain results for the amylose subunits alpha-D-glucose and maltose (alpha(1 -> 4) linked glucose dimer). The integral cross sections show double peaked broad structures between 8 eV and 20 eV similar to previously reported results for tetrahydrofuran and 2-deoxyribose, suggesting a general feature of molecules containing furanose and pyranose rings. These broad structures would reflect OH, CO and/or CC sigma* resonances, where inspection of low-lying virtual orbitals suggests significant contribution from sigma(OH)* anion states. Though we do not examine dissociation pathways, these anion states could play a role in dissociative electron attachment mechanisms, in case they were coupled to the long-lived pi* anions found in lignin subunits [de Oliveira et al., Phys. Rev. A, 2012, 86, 020701(R)]. Altogether, the resonance spectra of lignin, cellulose and hemicellulose components establish a physical-chemical basis for electron-induced biomass pretreatment that could be applied to biofuel production.

Physical Chemistry Chemical Physics 15[5], 1682-1689, 2013.

[P036-2013] "Magnetization reversal and exchange bias effects in hard/soft ferromagnetic bilayers with orthogonal anisotropies"

Navas, D.; **Torrejon, J.*; Beron, F.*;** Redondo, C.; Batallan, F.; Toperverg, B. P.; Devishvili, A.; Sierra, B.; Castano, F.; Pirota, K. R.; Ross, C. A.

The magnetization reversal processes are discussed for exchange-coupled ferromagnetic hard/soft bilayers made from Co0.66Cr0.22Pt0.12 (10 and 20 nm)/Ni (from 0 to 40 nm) films with out-of-plane and in-plane magnetic easy axes respectively, based on room temperature hysteresis loops and first-order reversal curve analysis. On increasing the Ni layer thicknesses, the easy axis of the bilayer reorients from out-of-plane to in-plane. An exchange bias effect, consisting of a shift of the in-plane minor hysteresis loops along the field axis, was observed at room temperature after in-plane saturation. This effect was associated with specific ferromagnetic domain configurations experimentally determined by polarized neutron reflectivity. On the other hand, perpendicular exchange bias effect was revealed from the out-of-plane hysteresis loops and it was attributed to residual domains in the magnetically hard layer.

New Journal of Physics 14, 113001, 2012.

[P037-2013] "Magnetostatic behaviour of antidot arrays under the local influence of nanopillars"

Beron F.*; Knobel M.*; Pirota K. R.*

We fabricated highly ordered patterned Permalloy nanometric structures by means of ion beam sputtering on top of an anodic aluminium oxide nanoporous template. First-order reversal curve (FORC) results and micromagnetic simulations indicate the presence of Permalloy inside one side of the pores, leading to a nanopillar array anisotropically arranged combined with an antidot array. The strong shape anisotropy of the pillar forces it to maintain the magnetization along its axis, even for a large in-plane applied field. This phenomenon induces out-of-plane hysteresis, as well as in-plane anisotropic behaviour. Depending on the in-plane applied field direction, the presence of nanopillars differently modifies the regular domain pattern, and therefore they could act as a new parameter for tailoring of magnetic anisotropy in antidot arrays.

Journal of Physics D-Applied Physics 45[50], 505002, 2012.

[P038-2013] "Measurement of electrons from semileptonic heavy-flavor hadron decays in pp collisions at root s=7 TeV"

Abelev, B.; Adam, J.; Adamova, D.; Adare, A. M.; Aggarwal, M. M.; **Chinellato, D. D.*; Dash, A.*; Takahashi, J.*;** et al.
ALICE Collaboration

The differential production cross section of electrons from semileptonic heavy-flavor hadron decays has been measured at midrapidity (\y\ < 0.5) in proton-proton collisions at root s = 7 TeV with ALICE at the LHC. Electrons were measured in the transverse momentum range 0.5 < p(t) < 8 GeV/c. Predictions from a fixed-order perturbative QCD calculation with next-to-leading-log resummation agree with the data within the theoretical and experimental uncertainties.

Physical Review D 86[11], 112007, 2012.

[P039-2013] "Measurement of prompt J/psi and beauty hadron production cross sections at mid-rapidity in pp collisions at root s=7 TeV"

Abelev, B.; Adam, J.; Adamova, D.; Adare, A. M.; Aggarwal, M. M.; **Chinellato, D. D.*; Dash, A.*; Takahashi, J.*; et al.**
ALICE Collaboration

The ALICE experiment at the LHC has studied J/psi production at mid-rapidity in pp collisions at root s = 7 TeV through its electron pair decay on a data sample corresponding to an integrated luminosity L-int = 5.6 nb(-1). The fraction of J/psi from the decay of long-lived beauty hadrons was determined for J/psi candidates with transverse momentum p(t) > 1,3 GeV/c and rapidity vertical bar y vertical bar < 0.9. The cross section for prompt J/psi mesons, i.e. directly produced J/psi and prompt decays of heavier charmonium states such as the psi(2S) and chi(c) resonances, is sigma(prompt J/psi) (p(t) > 1.3 GeV/c, vertical bar y vertical bar < 0.9) = 8.3 +/- 0.8(stat.) +/- 1.1 (syst.)(-1.4) (+1.5) (syst. pol.) mu b. The cross section for the production of b-hadrons decaying to J/psi with p(t) > 1.3 GeV/c and vertical bar y vertical bar < 0.9 is a sigma(J/psi <- hB) (p(t) > 1.3 GeV/c, vertical bar y vertical bar < 0.9) = 1.46 +/- 0.38 (stat.)(-0.32) (+0.26) (syst.) mu b. The results are compared to QCD model predictions. The shape of the p(t) and y distributions of b-quarks predicted by perturbative QCD model calculations are used to extrapolate the measured cross section to derive the b (b) over bar pair total cross section and d sigma/dy at mid-rapidity.

Journal of High Energy Physics [11], 065, 2012.

[P040-2013] "Measurement of the Cross Section for Electromagnetic Dissociation with Neutron Emission in Pb-Pb Collisions at root s(NN)=2.76 TeV"

Abelev, B.; Adam, J.; Adamova, D.; Adare, A. M.; Aggarwal, M. M.; **Chinellato, D. D.*; Dash, A.*; Takahashi, J.*; et al.**
ALICE Collaboration

The first measurement of neutron emission in electromagnetic dissociation of Pb-208 nuclei at the LHC is presented. The measurement is performed using the neutron zero degree calorimeters of the ALICE experiment, which detect neutral particles close to beam rapidity. The measured cross sections of single and mutual electromagnetic dissociation of Pb nuclei at root s(NN) = 2.76 TeV with neutron emission are sigma(singleEMD) = 187.4 +/- 0.2(stat)(-11.2)(+13.2) (syst) b and sigma(mutualEMD) = 5. 7 +/- 0.1(stat) +/- 0.4(syst) b, respectively. The experimental results are compared to the predictions from a relativistic electromagnetic dissociation model.

Physical Review Letters 109[25], 252302, 2012.

[P041-2013] "Neutral pion and eta meson production in proton-proton collisions at root s=0.9 TeV and root s=7 TeV"

Abelev, B.; Quintana, A. A.; Adamova, D.; Adare, A. M.; Aggarwal, M. M.; **Chinellato, D. D.*; Cosentino, M. R.*; Dash, A.*; Takahashi, J.***
ALICE Collaboration

The first measurements of the invariant differential cross sections of inclusive pi(0) and eta meson production at mid-rapidity in proton-proton collisions root s = 0.9 TeV and root s = 7 TeV are reported. The pi(0) measurement covers the ranges 0.4 < p(T) < 7 GeV/c and 0.3 < p(T) < 25 GeV/c for these two energies, respectively. The production of eta mesons was measured at root s = 7 TeV in the range 0.4 < p(T) < 15 GeV/c. Next-to-Leading Order perturbative QCD calculations, which are consistent with the pi(0) spectrum at root s = 0.9 TeV, overestimate those of pi(0) and eta mesons at root s = 7 TeV, but agree with the measured eta/pi(0) ratio at root s = 7 TeV.

Physics Letters B 717[1-3], 162-172, 2012.

[P042-2013] "Observables and unobservables in dark energy cosmologies"

Amendola, L.; Kunz, M.; **Motta, M.***; Saltas, I. D.; Sawicki, I.

The aim of this paper is to answer the following two questions: (1) Given cosmological observations of the expansion history and linear perturbations in a range of redshifts and scales as precise as is required, which of the properties of dark energy could actually be reconstructed without imposing any parameterization? (2) Are these observables sufficient to rule out not just a particular dark energy model, but the entire general class of viable models comprising a single scalar field? This paper bears both good and bad news. On one hand, we find that the goal of reconstructing dark energy models is fundamentally limited by the unobservability of the present values of the matter density Omega(m0), the perturbation normalization sigma(8) as well as the present matter power spectrum. On the other, we find that, under certain conditions, cosmological observations can nonetheless rule out the entire class of the most general single scalar-field models, i.e., those based on the Horndeski Lagrangian.

Physcal Review D 87[2], 023501, 2013.

[P043-2013] "On the unzipping of multiwalled carbon nanotubes"

dos Santos, R. P. B.; **Perim, E.*; Autreto, P. A. S.*; Brunetto, G.*; Galvao, D. S.***

Graphene nanoribbons (GNRs) are very interesting structures which can retain graphene's high carrier mobility while presenting a finite bandgap. These properties make GNRs very valuable materials for the building of nanodevices. Unzipping carbon nanotubes (CNTs) is considered one of the most promising approaches for GNR controlled and large-scale production, although some of the details of the CNT unzipping processes are not completely known. In this work we have investigated CNT unzipping processes through fully atomistic molecular dynamics simulations using reactive force fields (ReaxFF). Multiwalled CNTs of different dimensions and chiralities under induced mechanical stretching were considered. Our results show that fracture patterns and stress profiles are highly CNT chirality dependent. Our results also show that the 'crests' (partially unzipped CNT regions presenting high curvature), originating from defective CNT areas, can act as a guide for the unzipping processes, which can explain the almost perfectly linear cuts frequently observed in unzipped CNTs.

Nanotechnology 23[46], 465702, 2012.

[P044-2013] "pi-pi Interactions and magnetic properties in a series of hybrid inorganic-organic crystals"

Gonzalez, M.; Lemus-Santana, A. A.; Rodriguez-Hernandez, J.; **Knobel, M.***; Reguera, E.

The series of hybrid inorganic-organic solids T(Im)(2)[Ni(CN)(4)] with T = Fe, Co, Ni and Im = imidazole were prepared by soft chemical routes from aqueous solutions of the involved building units: imidazole, T2+ metal and the [Ni(CN)(4)](2-) anionic block. The obtained samples were characterized from infrared and UV-vis spectroscopies, and thermogravimetric, X-ray diffraction and magnetic measurements. Anhydrous solids which crystallize with a monoclinic unit cell, in the I2/a space group with four formula units per cell (Z=4) were obtained. Their crystal structure was solved ab initio from the recorded X-ray powder patterns and then refined by the Rietveld method. The metal T is found with octahedral coordination to four N ends of CN groups and two imidazole molecules while the inner Ni atom preserves its planar coordination. The system of layers remains stacked in an ordered 3D structure through dipole-dipole and pi-pi interactions between imidazole rings from neighboring layers. In this way, a pillared structure is achieved without requiring the coordination of both nitrogen atoms from imidazole ring. The recorded magnetic data indicate the occurrence of a predominant ferromagnetic interaction at low temperature for Co and Ni but not for Fe. Such magnetic ordering is more favorable for Ni with transition temperature of 14.67 K, which was ascribed to the relatively high polarizing power for this metal. Within the considered T metals, to nickel the highest electron-withdrawing ability corresponds and this leads to an increase for the metal-ligand electron clouds overlapping and to a stronger pi-pi attractive interaction, two factors that result into a higher magnetic ordering temperature.

Journal of Solid State Chemistry 197, 317-322, 2013.

[P045-2013] "Pion, Kaon, and Proton Production in Central Pb-Pb Collisions at root s(NN)=2.76 TeV"

Abelev, B.; Adam, J.; Adamova, D.; Adare, A. M.; Aggarwal, M. M.; **Chinellato, D. D.*; Dash, A.*; Takahashi, J.*; et al.**
ALICE Collaboration

In this Letter we report the first results on pi(+/-), K-+/-, p, and (p) over bar production at midrapidity (vertical bar y vertical bar < 0.5) in central Pb-Pb collisions at root s(NN) = 2.76 TeV, measured by the ALICE experiment at the LHC. The p(T) distributions and yields are compared to previous results at root s(NN) = 200 GeV and expectations from hydrodynamic and thermal models. The spectral shapes indicate a strong increase of the radial flow velocity with root s(NN), which in hydrodynamic models is expected as a consequence of the increasing particle density. While the K/pi ratio is in line with predictions from the thermal model, the p/pi ratio is found to be lower by a factor of about 1.5. This deviation from thermal model expectations is still to be understood.

Physical Review Letters 109[25], 252301, 2012.

[P046-2013] "Probing the stability of superheavy dark matter particles with high-energy neutrinos"

Esmaili, A.*; Ibarra, A.; **Peres, O. L. G.***

Two of the most fundamental properties of the dark matter particle, the mass and the lifetime, are nly weakly constrained by the astronomical and cosmological evidence of dark matter. We derive in this paper lower limits on the lifetime of dark matter particles with masses in the range 10 TeV - 10(15) TeV from the non-observation of ultrahigh energy neutrinos in the AMANDA, IceCube, Auger and ANITA experiments. For dark matter particles which produce neutrinos in a two body or a three body leptonic decay, we find that the dark matter lifetime must be longer than O(10(26) - 10(28)) s for masses between 10 TeV and the Grand Unification scale. Finally, we also calculate, for concrete particle physics scenarios, the limits on the strength of the interactions that induce the dark matter decay.

Journal of Cosmology and Astroparticle Physics [11], 034, 2012.

[P047-2013] " Production of K*(892)(0) and phi(1020) in pp collisions at root s=7 TeV"

Abelev, B.; Adam, J.; Adamova, D.; Adare, A. M.; Aggarwal, M. M.; **Chinellato, D. D.*; Dash, A.*; Takahashi, J.*, et al.**
ALICE Collaboration

The production of K*(892)(0) and phi(1020) in pp collisions at root s = 7 TeV was measured by the ALICE experiment at the LHC. The yields and the transverse momentum spectra d(2)N/dydp(T) at midrapidity vertical bar y vertical bar < 0.5 in the range 0 < p(T) < 6 GeV/c for K*(892)(0) and 0.4 < p(T) < 6 GeV/c for phi(1020) are reported and compared to model predictions. Using the yield of pions, kaons, and Omega baryons measured previously by ALICE at root s = 7 TeV, the ratios K*/K-, phi/K*, phi/ K-, phi/pi(-), and (Omega + <(Omega)over bar>)/phi are presented. The values of the K*/K-, phi/K* and phi/K- ratios are similar to those found at lower centre-of-mass energies. In contrast, the phi/pi(-) ratio, which has been observed to increase with energy, seems to saturate above 200 GeV. The (Omega + (Omega) over bar)/phi ratio in the p(T) range 1-5 GeV/ c is found to be in good agreement with the prediction of the HIJING/B (B) over bar v2.0model with a strong colour field.

European Physical Journal C 72[10], 2183, 2012.

[P048-2013] "Pseudogap in high-temperature superconductors from realistic Frohlich and Coulomb interactions"

Sica, G.; Samson, J. H.; **Alexandrov, A. S.***

It has been recently shown that the competition between unscreened Coulomb and Frohlich electron-phonon interactions can be described in terms of a short-range spin exchange J(p) and an effective on-site interaction (U) over tilde in the framework of the polaronic t-J(p)-(U) over tilde model. This model, that provides an explanation for high-temperature superconductivity in terms of Bose-Einstein condensation (BEC) of small and light bipolarons, is now studied as a charged Bose-Fermi mixture. Within this approximation, we show that a gap between bipolaron and unpaired polaron bands results in a strong suppression of low-temperature spin susceptibility, specific heat and tunnelling conductance, signalling the presence of a pseudogap regime in the normal state without any assumptions on pre-existing orders or broken symmetries in the normal state of the model.

EPL 100[3], 37005, 2012.

[P049-2013] "Simultaneous electroanalytical determination of hydroquinone and catechol in the presence of resorcinol at an SiO2/C electrode spin-coated with a thin film of Nb2O5"

Canevari, T. C.; Arenas L. T.; **Landers, R.***; Custodio, R.; Gushikem, Y.

This paper describes the development, characterization and application of an Nb2O5 film formed on the surface of a carbon ceramic material, SiO2/C, obtained by a sol-gel method, using the spin-coating technique. The working electrode using this material will be designated as SiCNb. Hydroquinone and catechol can be oxidized at this electrode in the presence of resorcinol, allowing their simultaneous detection. The electrochemical properties of the resulting electrode were investigated using cyclic and differential pulse voltammetry techniques. Well-defined and separated oxidation peaks were observed by differential pulse voltammetry in Tris-HCl buffer solution at pH 7 containing 1 mol L-1 KCl in the supporting electrolyte solution. The SiCNb electrode exhibited high sensitivity in the simultaneous determination of hydroquinone and catechol in the presence of resorcinol, with the limits of detection for hydroquinone and catechol being 1.6 mu mol L-1 and 0.8 mu mol L-1, respectively. Theoretical calculations were performed to determine the ionization energies of hydroquinone, catechol and resorcinol; the results were used to explain the simultaneous determination of species by differential pulse voltammetry. The presence of resorcinol did not produce any interference in the simultaneous detection of hydroquinone and catechol on the surface of the modified electrode.

Analyst 138[1], 315-324, 2013.

[P050-2013] "Spin injection in n-type resonant tunneling diodes"

Gordo, V. O.; Herval, L. K. S.; Galeti, H. V. A.; Gobato, Y. G.; **Brasil, M. J. S. P.***; Marques, G. E.; Henini, M.; Airey, R. J.

We have studied the polarized resolved photoluminescence of n-type GaAs/AlAs/GaAlAs resonant tunneling diodes under magnetic field parallel to the tunnel current. Under resonant tunneling conditions, we have observed two emission lines attributed to neutral (X) and negatively charged excitons (X-). We have observed a voltage-controlled circular polarization degree from the quantum well emission for both lines, with values up to -88% at 15 T at low voltages which are ascribed to an efficient spin injection from the 2D gases formed at the accumulation layers.

Nanoscale Research Letters 7, 592, 2012.

[P051-2013] "Spontaneous Periodic Diameter Oscillations in InP Nanowires: The Role of Interface Instabilities"

Oliveira, D. S.*; Tizei, L. H. G.*; Ugarte, D.*; Cotta, M. A.*

We have observed that thin InP nanowires generated by vapor-liquid-solid growth display spontaneous periodic diameter oscillations when large group III supersaturations are used. Diameter variations are associated with a large number of stacking faults and crystallographic phase changes(wurtzite/zinc-blende); also the axial distance between oscillations depends on the indium precursor flow used during the run. We attribute the morphology changes to a substantial deformation of the triple phase line (vapor-liquid-solid) at the catalyst nanoparticle edge originated from multistep nucleation during growth. The deformation alters the mechanical force balance acting on the nanoparticle during growth in such a way that the particle displaces from the nanowire top and wets the nanowire sidewall. Subsequently, as catalytic growth occurs at the sidewall, the associated increase in diameter will eventually push the NP back to its original wire-top position until the onset of a new instability at the triple phase line.

Nano Letters 13[1], 9-13, 2013.

[P052-2013] "Superhydrophobic polyethylcyanoacrylate coatings. Contact area with water measured by Raman spectral images, contact angle and Cassie-Baxter model"

Bonugli L. O.*; dos Santos M. V. P.*; de Souza E. F.; **Teschke O.***

Apolar fibers wired into a mesh-like microstructure forming a coating with a contact angle larger than 160 degrees and fabricated by polycyanoacrylate polymerization are described. Interconnected fibers with diameters measuring approximately 5 mu m are formed by texturized linear or folded nanowires. The structure forming the deposited film occupies similar to 1.5% of the coating's top geometric area. This value agrees with the water/coating contact area given by the Cassie-Baxter contact-angle model (similar to 1.5%). The spatial distribution of the surface in contact with water was determined by Raman spectral imaging (similar to 1.5%) using the polycyanoacrylate lines and by scanning electron microscopy (similar to 2.0%).

Journal of Colloid and Interface Science 388, 306-312, 2012.

[P053-2013] "Suppression of high transverse momentum D mesons in central Pb-Pb collisions at root s(NN)=2.76 TeV"

Abelev, B.; Adam, J.; Adamova, D.; Adare, A. M.; Aggarwal, M. M.; **Chinellato, D. D.*; Cosentino, M. R.*; Dash, A.*; Takahashi, J.*; et al.**
ALICE Collaboration

The production of the prompt charm mesons D-0, D+, D*(+), and their antiparticles, was measured with the ALICE detector in Pb-Pb collisions at the LHC, at a centre-of-mass energy root s(NN) = 2.76 TeV per nucleon-nucleon collision. The p(t)-differential production yields in the range 2 < p(t) < 16 GeV/c at central rapidity, vertical bar y vertical bar < 0.5, were used to calculate the nuclear modification factor R-AA with respect to a proton-proton reference obtained from the cross section measured at root s = 7 TeV and scaled to root s = 2.76 TeV. For the three meson species, R-AA shows a suppression by a factor 3-4, for transverse momenta larger than 5 GeV/c in the 20% most central collisions. The suppression is reduced for peripheral collisions.

Journal of High Energy Physics [9], 112, 2012.

[P054-2013] "Surface Modification of Polycarbonate by Atmospheric-Pressure Plasma Jets"

Mello, C. B.; Kostov, K. G.; **Machida, M.***; Hein, L. R. O. D.; de Campos, K. A.

Plasmas have been frequently employed to modify material surface properties; however, many of these processes are not suitable for treating sensitive materials and biological objects that cannot withstand vacuum and/or high temperature. Atmospheric-pressure plasma jets (APPJs) using inert gases can be easily adapted for this purpose since they exhibit high plasma stability, efficient reaction chemistry, and low temperature. In this paper, an APPJ with simple configuration was designed and applied for surface treatment of polycarbonate (PC) films. Optical emission spectroscopy was used to identify the excited plasma species presented inside the device and in the plasma plume. Material characterization was carried out by water contact angle measurements and atomic force microscopy. The interaction of the plasma jet with the PC samples resulted in a rougher surface and enhanced wettability.

IEEE Transactions on Plasma Science 40[11], SI, 2800-2805, Parte 1, 2012.

[P055-2013] "Synchronization of Micromechanical Oscillators Using Light"

Zhang, M. A.; **Wiederhecker, G. S.***; Manipatruni, S.; Barnard, A.; McEuen, P.; Lipson, M.

Synchronization, the emergence of spontaneous order in coupled systems, is of fundamental importance in both physical and biological systems. We demonstrate the synchronization of two dissimilar silicon nitride micromechanical oscillators, that are spaced apart by a few hundred nanometers and are coupled through an optical cavity radiation field. The tunability of the optical coupling between the oscillators enables one to externally control the dynamics and switch between coupled and individual oscillation states. These results pave a path toward reconfigurable synchronized oscillator networks.

Physical Review Letters 109[23], 233906, 2012.

[P056-2013] "The rapid atmospheric monitoring system of the Pierre Auger Observatory"

Abreu, P.; Aglietta, M.; Ahlers, M.; Ahn, E. J.; Albuquerque, I. F. M.; Allard, D.; **Alves Batista, R.*; Chinellato, J. A.*; Daniel, B.*; de Mello Junior, W. J. M.*; Dobrigkeit, C.*; Escobar, C. O.*; Fauth, A. C.*; Kemp, E.*; Muller, M. A.*; Selmi-Dei, D. Pakk*; Zimbres S. M.*; et al.**
Pierre Auger Collaboration

The Pierre Auger Observatory is a facility built to detect air showers produced by cosmic rays above 10(17) eV. During clear nights with a low illuminated moon fraction, the UV fluorescence light produced by air showers is recorded by optical telescopes at the Observatory. To correct the observations for variations in atmospheric conditions, atmospheric monitoring is performed at regular intervals ranging from several minutes (for cloud identification) to several hours (for aerosol conditions) to several days (for vertical profiles of temperature, pressure, and humidity). In 2009, the monitoring program was upgraded to allow for additional targeted measurements of atmospheric conditions shortly after the detection of air showers of special interest, e. g., showers produced by very high-energy cosmic rays or showers with atypical longitudinal profiles. The former events are of particular importance for the determination of the energy scale of the Observatory, and the latter are characteristic of unusual air shower physics or exotic primary particle types. The purpose of targeted (or "rapid") monitoring is to improve the resolution of the atmospheric measurements for such events. In this paper, we report on the implementation of the rapid monitoring program and its current status. The rapid monitoring data have been analyzed and applied to the reconstruction of air showers of high interest, and indicate that the air fluorescence measurements affected by clouds and aerosols are effectively corrected using measurements from the regular atmospheric monitoring program. We find that the rapid monitoring program has potential for supporting dedicated physics analyses beyond the standard event reconstruction.

Journal of Instrumentation 7, P09001, 2012.

[P057-2013] "Thermal Effusivity and Thermal Conductivity of Biodiesel/Diesel and Alcohol/Water Mixtures"

Guimaraes, A. O.; Machado, F. A. L.; da Silva, E. C.; **Mansanares, A. M.***

The photopyroelectric (PPE) technique was used for the determination of the thermal effusivity and thermal conductivity of biodiesel in diesel and other binary liquid mixtures, precisely, ethanol, and ethylene glycol in water. The front configuration (FPPE) has been explored in the frequency scan approach for obtaining thermal-effusivity values. Measurements show good reproducibility, with uncertainties around 1 % to 2 %, and the results for reference samples, such as ethanol and water, are in good agreement with literature values. The thermal-conductivity values of all samples were determined using the thermal-effusivity data presented here and the thermal-diffusivity data of exactly the same set of samples, reported elsewhere. Based on these results, the different strengths in the molecular interactions related to the several mixtures were evidenced, as proposed by Dadarlat et al. It was shown that, indeed, the thermal effusivity is the property presenting the smallest sensitivity for the molecular association phenomenon, while the thermal conductivity presents an intermediate sensitivity. Nevertheless, the analysis of both properties revealed the existence of weak cohesive interactions among the hydrocarbons of diesel and the esters of biodiesel.

International Journal of Thermophysics 33[10-11], SI, 1842-1847, 2012.

[P058-2013] "Thermal Properties of Biodiesel and Their Corresponding Precursor Vegetable Oils Obtained by Photopyroelectric Methodology"

Machado, F. A. L.; Zanelato, E. B.; Guimaraes, A. O.; da Silva, E. C.; **Mansanares, A. M.***

The photopyroelectric technique (PPE) was used for thermal characterization of biodiesel and their corresponding precursor vegetable oils. Different configurations of PPE were applied in these studies. The standard and inverse configurations allowed the determination of the thermal diffusivity (alpha) and thermal effusivity (e), respectively. From these two parameters the thermal conductivity was calculated. Measurements were performed for reference samples (water and ethylene glycol), biodiesel, and some corresponding precursor vegetable oils. The experiments showed good reproducibility, with uncertainties around 1 % to 2 % for all the samples. Lower values for both alpha and e of the biodiesel when compared to their corresponding precursor vegetable oils were observed, indicating that these thermophysical properties were sensitive to structural changes during the transesterification process.

International Journal of Thermophysics 33[10-11], SI, 1848-1855, 2012.

[P059-2013] "Thermal Stability and Ordering Study of Long- and Short-Alkyl Chain Phosphonic Acid Multilayers"

de Pauli, M.*; Prado, M. D.; Matos, M. J. S.; Fontes, G. N.; Perez, C. A.; Mazzoni, M. S. C.; Neves, B. R. A.; Malachias, A.

Long-range order evolution of self-assembled phosphonic acid multilayers as a function of temperature is studied here for two molecules with different alkyl chain length. By using synchrotron conventional diffraction, distinct order configurations are retrieved on phosphonic acid multilayers and their thermodynamic behavior monitored by energy-dispersive diffraction. This later technique allows us to observe the system behavior near order-disorder temperatures, as well as to determine the most stable configurations in the range from room temperature up to 120 degrees C. Planar order is also addressed by wide-angle X-ray scattering (WAXS) transmission experiments. Order parameter phase diagrams are built based on the experimental results, showing the dominant configuration at each temperature. The multilayer molecular long-range order retrieved from the experiments is corroborated by first principles calculations based on the Density Functional Theory. The bulk configurations depicted in this work are produced by molecule-molecule interactions and allow for future comparisons with the behavior of ordered molecules in few-monolayers configurations, commonly used in organic devices, where the presence of surfaces and interfaces strongly affects the molecule packing.

Langmuir 28[43], 15124-15133, 2012.

[P060-2013] "Total Hadronic Cross-Section Data and the Froissart-Martin Bound"

Fagundes, D. A.*; Menon, M. J.*; Silva, P. V. R. G.*

The energy dependence of the total hadronic cross section at high energies is investigated with focus on the recent experimental result by the Total Elastic and Diffractive Cross-section Measurement Collaboration at 7 TeV and the Froissart-Martin bound. On the basis of a class of analytical parametrization with the exponent gamma in the leading logarithm contribution as a free parameter, different variants of fits to pp and p total cross-section data above 5 GeV are developed. Two ensembles are considered, the first comprising data up to 1.8 TeV and the second also including the data collected at 7 TeV. We show that in all fit variants applied to the first ensemble, the exponent is statistically consistent with gamma = 2. Applied to the second ensemble, however, the same variants yield gamma values above 2, a result already obtained in two other analysis, by Amaldi et al. and by the UA4/2 Collaboration. As recently discussed by Azimov, this faster-than-squared-logarithm rise does not necessarily violate unitarity. Our results suggest that the energy dependence of the hadronic total cross section at high energies still constitutes an open problem.

Brazilian Journal of Physics 42[5-6], 452-464, 2012.

[P061-2013] "Transverse sphericity of primary charged particles in minimum bias proton-proton collisions at root s=0.9, 2.76 and 7 TeV"

Abelev, B.; Adam, J.; Adamova, D.; Adare, A. M.; Aggarwal, M. M.; **Chinellato, D. D.*; Cosentino, M. R.*; Dash, A.*; Takahashi, J.*; et al.**
ALICE Collaboration

Measurements of the sphericity of primary charged particles in minimum bias proton-proton collisions at root s = 0.9, 2.76 and 7 TeV with the ALICE detector at the LHC are presented. The observable is measured in the plane perpendicular to the beam direction using primary charged tracks with p(T) > 0.5 GeV/c in vertical bar eta vertical bar < 0.8. The mean sphericity as a function of the charged particle multiplicity at mid-rapidity (N-ch) is reported for events with different p(T) scales ("soft" and "hard") defined by the transverse momentum of the leading particle. In addition, the mean charged particle transverse momentum versus multiplicity is presented for the different event classes, and the sphericity distributions in bins of multiplicity are presented. The data are compared with calculations of standard Monte Carlo event generators. The transverse sphericity is found to grow with multiplicity at all collision energies, with a steeper rise at low N-ch, whereas the event generators show an opposite tendency. The combined study of the sphericity and the mean p(T) with multiplicity indicates that most of the tested event generators produce events with higher multiplicity by generating more back-to-back jets resulting in decreased sphericity (and isotropy). The PYTHIA6 generator with tune PERUGIA-2011 exhibits a noticeable improvement in describing the data, compared to the other tested generators.

European Physical Journal C 72[9], 2124, 2012.

[P062-2013] "Tuning resistive switching on single-pulse doped multilayer memristors"

Siles, P. F.; **de Pauli, M.***; Bufon, C. C. B.; Ferreira, S. O.; Bettini, J.; Schmidt, O. G.; Malachias, A.

Short-period multilayers containing ultrathin atomic layers of Al embedded in titanium dioxide (TiO2) film-here called single-pulse doped multilayers-are fabricated by atomic layer deposition (ALD) growth methods. The approach explored here is to use Al atoms through single-pulsed deposition to locally modify the chemical environment of TiO2 films, establishing a chemical control over the resistive switching properties of metal/oxide/metal devices. We show that this simple methodology can be employed to produce well-defined and controlled electrical characteristics on oxide thin films without compound segregation. The increase in volume of the embedded Al2O3 plays a crucial role in tuning the conductance of devices, as well as the switching bias. The stacking of these oxide compounds and their use in electrical devices is investigated with respect to possible crystalline phases and local compound formation via chemical recombination. It is shown that our method can be used to produce compounds that cannot be synthesized a priori by direct ALD growth procedures but are of interest due to specific properties such as thermal or chemical stability, electrical resistivity or electric field polarization possibilities. The monolayer doping discussed here impacts considerably on the broadening of the spectrum of performance and technological applications of ALD-based memristors, allowing for additional degrees of freedom in the engineering of oxide devices. S Online supplementary data available from stacks.iop.org/Nano/24/035702/mmedia

Nanotechnology 24[3], 035702, 2013.

[P063-2013] "Turing patterns and apparent competition in predator-prey food webs on networks"

Fernandes, L. D.*; de Aguiar, M. A. M.*

Reaction-diffusion systems may lead to the formation of steady-state heterogeneous spatial patterns, known as Turing patterns. Their mathematical formulation is important for the study of pattern formation in general and plays central roles in many fields of biology, such as ecology and morphogenesis. Here we show that Turing patterns may have a decisive role in shaping the abundance distribution of predators and prey living in patchy landscapes. We extend the original model proposed by Nakao and Mikhailov [Nat. Phys. 6, 544 (2010)] by considering food chains with several interacting pairs of prey and predators distributed on a scale-free network of patches. We identify patterns of species distribution displaying high degrees of apparent competition driven by Turing instabilities. Our results provide further indication that differences in abundance distribution among patches can be generated dynamically by self organized Turing patterns and not only by intrinsic environmental heterogeneity.

Physical Review E 86[5], 056203, Parte 1, 2012.

[P064-2013] "Two-Dimensional Magnetic Correlations and Partial Long-Range Order in Geometrically Frustrated Sr2YRuO6"

Granado, E.*; Lynn, J. W.; Jardim, R. F.; Torikachvili, M. S.

Neutron diffraction on the double perovskite Sr2YRuO6 with a quasi-fcc lattice of Ru moments reveals planar magnetic correlations that condense into a partial long-range ordered state with coupled alternate antiferromagnetic (AFM) YRuO4 square layers coexisting with the short-range correlations below T-N1 = 32 K. A second transition to a fully ordered AFM state below T-N2 = 24 K is observed. The reduced dimensionality of the spin correlations is arguably due to a cancellation of the magnetic coupling between consecutive AFM square layers in fcc antiferromagnets, which is the simplest three-dimensional frustrated magnet model system.

Physical Review Letters 110[1], 017202, 2013.

[P065-2013] "Variations of the muon flux at sea Level Associated with Interplanetary ICMEs and Corotating Interaction Regions"

Augusto, C. R. A.; Kopenkin, V.; Navia, C. E.; Tsui, K. H.; Shigueoka, H.; **Fauth, A. C.*; Kemp, E.*; Manganote, E. J. T.***; de Oliveira M. A. L; Miranda P.; Ticona R.; Velarde A.

We present the results of an ongoing survey on the association between the muon flux variation at ground level (3 m above sea level) registered by the Tupi telescopes (Niteri-Brazil, 22 degrees.9S, 43 degrees.2W, 3 m) and the Earth-directed transient disturbances in the interplanetary medium propagating from the Sun (such as coronal mass ejections (CME), and corotating interaction regions (CIRs)). Their location inside the South Atlantic Anomaly region enables the muon telescopes to achieve a low rigidity of response to primary and secondary charged particles. The present study is primarily based on experimental events obtained by the Tupi telescopes in the period from 2010 August to 2011 December. This time period corresponds to the rising phase of solar cycle 24. The Tupi events are studied in correlation with data obtained by space-borne detectors (SOHO, ACE, GOES). Identification of interplanetary structures and associated solar activity was based on the nomenclature and definitions given by the satellite observations, including an incomplete list of possible interplanetary shocks observed by the CELIAS/MTOF Proton Monitor on the Solar and Heliospheric Observatory (SOHO) spacecraft. Among 29 experimental events reported in the present analysis, there are 15 possibly associated with the CMEs and sheaths, and 3 events with the CIRs (forward or reverse shocks); the origin of the remaining 11 events has not been determined by the satellite detectors. We compare the observed time (delayed or anticipated) of the muon excess (positive or negative) signal on Earth (the Tupi telescopes) with the trigger time of the interplanetary disturbances registered by the satellites located at Lagrange point L1 (SOHO and ACE). The temporal correlation of the observed ground-based events with solar transient events detected by spacecraft suggests a real physical connection between them. We found that the majority of observed events detected by the Tupi experiment were delayed in relation to the satellite triggers. This result agrees with theoretical expectations. Our experimental data indicate that the Tupi experiment is able to add new information and can be complementary to other techniques designed to interpret the origin of some interplanetary disturbances observed by satellites.

Astrophysical Journal 759[2], 143, 2012.

Proceedings

[P066-2013] "Spectral bandwidth analysis of high sensitivity refractive index sensor based on multimode interference fiber device"

Pachon, E. G. P.*; Franco, M. A. R.; **Cordeiro, C. M. B.***; Liao, Y.(Ed.); Jin, W.(Ed.); Sampson, D. D.(Ed.); Yamauchi, R.(Ed.); Chung, Y.(Ed.); Nakamura, K.(Ed.); Rao, Y. (Ed.)

Fiber optic structures based on multimode interference were investigated to the refractive index (RI) sensing. The proposed device is a singlemode-multimode-singlemode (SMS) structure, where the multimode section is a coreless fiber (MMF). The numerical analyses were carried out by beam propagation and modal expansion methods. Ultra-high sensitivity was obtained: 827 nm/RIU over a RI range of 1.30-1.44 and a maximum sensitivity of 3500 nm/RIU for RI similar to 1.43, considering Delta(RI) = 0.01. The dependence of spectral bandwidth was investigated taking into account the multimode fiber diameter and the coupling efficiency between modes at the input junction singlemode-multimode.

In: INTERNATIONAL CONFERENCE ON OPTICAL FIBER SENSORS (OFS), 22., 2012, Beijing. Proceeding. Bellingham: Spie-int Soc Optical Engineering, 2012. v. 8421, 84217Q.

Correções

"Applications of a granular model and percolation theory to the electrical resistivity of heat treated endocarp of babassu nut (vol 25, pg 417, 1987)"

Emmerich, F. G.; de Sousa, J. C.; Torriani, I. L.; **Luengo, C. A.***

Carbon 51, 439-439, 2013.

"Pseudogap in high-temperature superconductors from realistic Frohlich and Coulomb interactions (vol 100, 37005, 2012)"

Sica, G.; Samson, J. H.; **Alexandrov, A. S.***

EPL 100[5], 59901, 2012.

*** Autores do Instituto de Física "Gleb Wataghin" - IFGW**

Defesas de Dissertações - Mestrado

[D001-13] "Mecanismo de Pontecorvo Estendido"

Aluno: Eduardo Marcio Zavanin

Orientador: Marcelo Moraes Guzzo

Fevereiro/2013

Defesas de Teses - Doutorado

[T001-13] "Fenomenologia de neutrinos massivos em cosmologia"

Aluno: Daniel Francisco Boriero

Orientador: Pedro Cunha de Holanda

Fevereiro/2013

[T002-13] "Propagação Semiclássica na representação de estados coerentes"

Aluno: Thiago de Freitas Viscondi

Orientador: Marcus Aloizio Martinez de Aguiar

Fevereiro/2013

Fonte: Portal IFGW/Pós-graduação.
Disponível em: http://portal.ifi.unicamp.br/eventos/eventos-defesas-tese

*** Acesse o portal Abstracta <http://abstracta.ifi.unicamp.br>** e faça seu **cadastro como Leitor** para receber as novidades de cada novo número publicado.

Abstracta

Instituto de Física
Diretor: Prof. Dr. Daniel Pereira
Universidade Estadual de Campinas - UNICAMP
Cidade Universitária Zeferino Vaz
13083-859 - Campinas - SP - Brasil
e-mail: secdir@ifi.unicamp.br
Fone: 0XX 19 3521-5300

Publicação

Biblioteca do Instituto de Física Gleb Wataghin
http://portal.ifi.unicamp.br/biblioteca
Diretora Técnica: Sandra Maria Carlos Cartaxo

Elaboração
Maria Graciele Trevisan
graciele@ifi.unicamp.br

Projeto Gráfico
ÍgneaDesign

Impressão

Gráfica Central - Unicamp